Progress in Fractional Differentiation and Applications
An International Journal

http://dx.doi.org/10.18576/pfda/120113

Control and Mitigation Strategies for Fractional Order ENSO Model via Artificial Neural Network Approach

Jagdev Singh[1,*], *Rakesh Saini*[1], *Dumitru Baleanu*[2] *and Devendra Kumar*[3]

[1] Department of Mathematics, JECRC University, Jaipur-303905, Rajasthan, India
[2] Department of Computer Science and Mathematics, Lebanese American University, Beirut, Lebanon
[3] Department of Mathematics, University of Rajasthan, Jaipur-302004, Rajasthan, India

Received: 11 Nov. 2025, Revised: 2 Dec. 2025, Accepted: 22 Dec. 2025
Published online: 1 Jan. 2026

Abstract: The current investigation is related to solve the fractional El Niño-Southern Oscillation (ENSO) model by using the Gudermannian neural network approach. The network weights are optimized using a hybrid genetic algorithm with an interior point algorithm (GAIPA). An error function is defined for ENSO with its initial conditions and optimized its weights using GAIPA. Classical and fractional order ENSO models are solved with different parameter values. The convergence measures in the sense of root mean square error (RMSE), mean absolute deviation (MAD), and Theil's inequality coefficient (TIC) are also discussed and prove the effectiveness of the proposed method.

Keywords: ENSO model, Artificial neural network, Gudermannian neural network, Genetic algorithm, Interior point algorithm.

1 Introduction

The El Niño-Southern Oscillation (ENSO) is a prominent and influential climate phenomenon that is characterized by fluctuations in sea surface temperatures and atmospheric conditions in the tropical Pacific Ocean. ENSO significantly impacts on global weather patterns that contributes to various climatic events such as droughts, floods, and hurricanes. It has two primary phases, El Niño and La Niña, that represent the two opposite extremes of oceanic and atmospheric interactions. El Niño is associated with warming sea surface temperatures, while La Niña features cooling effects. Understanding ENSO is crucial for climate prediction and disaster preparedness, as its effects resonate through ecosystems, biodiversity, agriculture, public health, economies, and infrastructure worldwide. For more details about ENSO, see [1–8].

Rao and Sperber [9] simulated the coupled El Niño Southern Oscillation model. Wang [10] developed a unified oscillator model for the ENSO phenomenon. This model has significant implications for understanding ENSO dynamics and its relationship with other existing models. Notable among these are the delayed oscillator model, the western Pacific oscillator model, the recharge discharge oscillator model, and the advective-reflective oscillator model. Wei et. al. [11] investigated the relationship between ENSO and various financial markets, including carbon emission allowance, crude oil, and renewable energy stocks, using a TVP-VAR model. The authors analyzed time and frequency domain evidence to find out the relationships between these factors. Maher et. al. [12] studied the future dynamics of El Niño-Southern Oscillation using large ensembles, revealing varying responses and model disparities. Through diverse model outputs, it illuminates how ENSO behavior evolves under different climate scenarios, offering insights into potential impacts and uncertainties. The contribution of atmospheric transport on ENSO was described by Baier et. al. [13]. The authors also show the effect of atmospheric transport on the global weather system and energy transportation. The effects of ENSO on global runoff are reported by You et. al. [14].

* Corresponding author e-mail: jagdevsinghrathore@gmail.com

Fractional calculus is a fascinating and rapidly evolving field of mathematics that extends the concept of derivatives and integrals to non-integer orders [15–18]. Classical calculus focuses on classical orders of differentiation and integration, while fractional calculus generalizes these operations to arbitrary orders [15–19]. This expansion opens up a rich landscape of theoretical and practical applications, connecting deeply with various scientific and engineering disciplines [15–19]. Pinto and Carvalho [20] studied the arbitrary-order HIV infection model. For Banach space valued functions, Anastassiou [21] developed left fractional calculus theory. Losada and Nieto [22] presented the properties of the Caputo-Fabrizio fractional derivative. Kumar et. al. [23] solved a two-species predator-prey model by utilizing the Bernstein wavelet and Euler methods. Jafari and Gejji [24] solved the nonlinear system of arbitrary order differential equations by using Adomian decomposition. The impact of vaccination on the dynamics of COVID-19 viral infection was studied by Jan et. al. [25] in a fractional framework. Fractional integrals and derivatives of some elementary functions are evaluated by Garrappa et. al. [26]. Rezapour et. al. [27] analyzed the anthrax disease model in animals based on Caputo-Fabrizio fractional derivative. Cai and Li [28] reviewed the numerical approximations of fractional derivatives and integrals. Kumar et. al. [29] numerically solved the non-integer order mathematical model with a nonsingular kernel for thrombin receptor activation in calcium signals. A numerical scheme was presented by Kumar et. al. [30] to analyze the fractional Lienard's equation. A numerical algorithm was presented by Kumar et. al. [31] to solve the time-fractional Black–Scholes model with the utilization of the homotopy perturbation method and homotopy analysis method. Singh et. al. [32] examined the fractional smoking model using a new fractional derivative with a non-singular kernel and reported the effect of various parameters.

ENSO models have relied on integer-order differential equations to simulate the complex interactions between the ocean and the atmosphere. However, recent advances have introduced the concept of fractional calculus into climate modeling, leading to the development of the fractional El Niño-Southern Oscillation (FENSO) model [33–35]. Fractional calculus, which extends the notion of derivatives and integrals to non-integer orders, provides a more flexible framework for capturing memory effects and anomalous diffusion processes inherent in climatic systems [33–37].

Singh et. al. [33] analyzed ENSO model by using a novel fractional derivative, the Caputo-Fabrizio fractional derivative. The authors also examined the existence and uniqueness of the solution. Gómez-Aguilar [38] investigated the Vallis model for ENSO and identified various stable states and periodic cycles, which enhances comprehension of ENSO's dynamics and variability. Zhang et. al. [34] reported the effects of fractional operator on the ENSO model. The authors elaborated the equilibrium points with stability, existence of solution, uniqueness, and strength of the solution. Also, for some fractional orders, complex dynamics are presented.

Mall and Chakraverty [39] studied the Legendre neural network to solve classical order initial and boundary value problems. Jafarian et. al. [40] utilized an artificial neural network procedure to solve a class of arbitrary order initial value problems. Sabir et. al. [41] proposed an artificial neural network algorithm, the Meyer wavelet neural networks algorithm, to solve fractional Lane-Emden systems and also compare the results with the exact solution and show the strength of the proposed method. Sabir et. al. [42] solve the corneal shape model that is used in eye surgery with the utilization of the Gudermannian neural network. Ahmad et. al. [43] solved the higher-order boundary value problem (BVP) arising in induction motor using the artificial neural network algorithm. The authors used the radial basis function as an activation function. Rasanan et. al. [44] designed the fractional orthogonal neural network to solve the Lane-Emden equation. The authors used the fractional Legendre function as an activation function for the hidden layer. Saneifard et. al. [45] solved a fractional order linear Volterra-type differential equation in two dimensions by utilizing the extension of the artificial neural network technique. Khan et. al. [46] solved nonlinear multiorder fractional differential equations by utilizing the backpropagated Levenberg-Marquardt algorithm dependent neural network. Raja et. al. [47] utilized artificial neural networks and sequential quadratic programming to solve the nonlinear quadratic fractional Riccati differential equation.

The traditional way to solve fractional differential equations is highly complicated. One such equation is the fractional ENSO model. Many analytic and numerical methods have been derived to solve the fractional ENSO model [33, 38]. Zeng [48] used the Laplace-Adomian-Pade technique to approximate the solution of the ENSO model. Different approaches have their own merits and demerits, while Gudermannian neural network procedures have not yet been exploited to solve the fractional El Niño Southern Oscillation system. The general form of the fractional ENSO model is represented as follows [33].

$$\begin{cases} {}_0D_t^r P = aP + bQ - cP^3 \\ {}_0D_t^r Q = -dP - eQ \end{cases} \tag{1}$$

with the initial conditions $P(0) = 1, Q(0) = 1$
where a, b, c, d, and e are constants that represent the physical properties of the ENSO model and e is a perturbation

coefficient that is defined on $(0,1)$ and small ample. P and Q are real-valued functions, P represents the sea surface temperature, and Q represents the thermo-cline depth anomaly of the eastern equatorial Pacific ocean.
An artificial neural network, the Gudermannian neural network (GNN), has been designed and optimized by a hybrid genetic algorithm (GA) and interior point algorithm (IPA), i.e., GNN-GAIPA. Two cases of the ENSO model are discussed here: integer order and fractional order. The results are compared with the exact solution for case 1 and case 2 compared with the solution obtained by the fractional Euler method [FEM] [49].
The structure of the paper is as follows. Section 2 contains the proposed methodology for formulating the Gudermannian neural network and optimizations with the GAIPA algorithm. The performance of the proposed method is presented in Section 3. Section 4 contains the numerical outcomes of the presented method. Conclusion have been discussed in Section 5.

2 Proposed Methodology

The GNN is designed to solve the fractional ENSO model in this section. Formulation of the fractional ENSO system together with fitness function and optimization process based on GAIPA is described here.

2.1 Gedernmanian Neural Network

The notations for the proposed method are used as follows. The approximate solution is represented as $\begin{bmatrix}\hat{P}\\ \hat{Q}\end{bmatrix}$ and its fractional order derivative is represented as $\begin{bmatrix}D^r\hat{P}\\ D^r\hat{Q}\end{bmatrix}$. For m number of neurons, the expression of neural networks are expressed as

$$\begin{bmatrix}\hat{P}\\ \hat{Q}\end{bmatrix} = \begin{bmatrix}\sum_{i=0}^{m}\theta_{P,i}f(\lambda_{P,i}x+\gamma_{P,i})\\ \sum_{i=0}^{m}\theta_{Q,i}f(\lambda_{Q,i}x+\gamma_{Q,i})\end{bmatrix} \tag{2}$$

The fractional derivative of order r of Eq. (2) is

$$\begin{bmatrix}D^r\hat{P}\\ D^r\hat{Q}\end{bmatrix} = \begin{bmatrix}\sum_{i=0}^{m}\theta_{P,i}D^r f(\lambda_{P,i}x+\gamma_{P,i})\\ \sum_{i=0}^{m}\theta_{Q,i}D^r f(\lambda_{Q,i}x+\gamma_{Q,i})\end{bmatrix} \tag{3}$$

The unknown weights of the proposed network are represented by A, which is noted as follows

$$A = [A_P, A_Q]$$

Where $A_P = [\theta_P, \lambda_P, \gamma_P]$ and $A_Q = [\theta_Q, \lambda_Q, \gamma_Q]$ where
$\theta_{\mathbf{P}} = [\theta_{P,1}, \theta_{P,2}, \cdots, \theta_{P,m}]$,
$\lambda_{\mathbf{P}} = [\lambda_{P,1}, \lambda_{P,2}, \cdots, \lambda_{P,m}]$,
$\gamma_{\mathbf{P}} = [\gamma_{P,1}, \gamma_{P,2}, \cdots, \gamma_{P,m}]$,
$\theta_{\mathbf{Q}} = [\theta_{Q,1}, \theta_{Q,2}, \cdots, \theta_{Q,m}]$,
$\lambda_{\mathbf{Q}} = [\lambda_{Q,1}, \lambda_{Q,2}, \cdots, \lambda_{Q,m}]$,
$\gamma_{\mathbf{Q}} = [\gamma_{Q,1}, \gamma_{Q,2}, \cdots, \gamma_{Q,m}]$.

The Gudermannian kernel is defined as

$$f(x) = 2tan^{-1}(e^x) - \frac{\pi}{2} \tag{4}$$

Using Gudermannian kernel Eq. (4) in the proposed network given by Eq. (2) and Eq. (3), we have

$$\begin{bmatrix}\hat{P}\\ \hat{Q}\end{bmatrix} = \begin{bmatrix}\sum_{i=0}^{m}\theta_{P,i}(2tan^{-1}(e^{(\lambda_{P,i}x+\gamma_{P,i})}) - \frac{\pi}{2})\\ \sum_{i=0}^{m}\theta_{Q,i}(2tan^{-1}(e^{(\lambda_{Q,i}x+\gamma_{Q,i})}) - \frac{\pi}{2})\end{bmatrix} \tag{5}$$

and

$$\begin{bmatrix} D^r\hat{P} \\ D^r\hat{Q} \end{bmatrix} = \begin{bmatrix} \sum_{i=0}^{m} \theta_{P,i} D^r (2tan^{-1}(e^{(\lambda_{P,i}x+\gamma_{P,i})}) - \frac{\pi}{2}) \\ \sum_{i=0}^{m} \theta_{Q,i} D^r (2tan^{-1}(e^{(\lambda_{Q,i}x+\gamma_{Q,i})}) - \frac{\pi}{2}) \end{bmatrix} \tag{6}$$

To approximate the weights of the GNN, one may formulate an error function as follows

$$E = E_1 + E_2 + E_3 + E_4. \tag{7}$$

Where

$$E_1 = \frac{1}{N}\sum_{j=1}^{N} [D^r\hat{P}_j - a\hat{P}_j - b\hat{Q}_j + c\hat{P}_j^3]^2. \tag{8}$$

$$E_2 = [\hat{P}_0 - P(0)]^2. \tag{9}$$

$$E_3 = \frac{1}{N}\sum_{j=1}^{N} [D^r\hat{Q}_j + d\hat{P}_j + e\hat{Q}_j]^2. \tag{10}$$

$$E_4 = [\hat{Q}_0 - Q(0)]^2. \tag{11}$$

Where $N = \frac{1}{h}$, $\hat{P}_j = \hat{P}(x_j)$, $\hat{Q}_j = \hat{Q}(x_j)$, $x_j = jh$. As the error function E (Eq. 7) tends to 0, the approximate solution $\begin{bmatrix} \hat{P} \\ \hat{Q} \end{bmatrix}$ tends to the exact solution $\begin{bmatrix} P \\ Q \end{bmatrix}$.

2.2 Network Optimization

One may determine the weights of the network using the hybridization of the Ganatic algorithm with the Interior Point Algorithm (GAIPA). The pseudocode of the Gudermannian neural network for the fractional ENSO model is shown in Table 1.

The genetic algorithm (GA) is based on a natural genetic process that is used to optimize the constrained / unconstrained optimization problem. GA can solve a variety of complex problems. GA uses crossover and mutation to find out the optimal solution. Its effectiveness depends on mutation, crossover, and selection. Its optimization strength may be improved via the hybridization of the local search algorithm. Genetic algorithms have wildly usage in the optimization process, some of them are as follows. Cavallaro et. al. [50] used a genetic algorithm in image reconstruction. Li et. al. [51] presented a genetic algorithm to optimize the circuitry of tube-fin heat exchangers in air-conditioning and heat pump applications. Delwar et. al. [52] designed a power amplifier for usage in 5G applications that was based on an adaptive genetic algorithm. GA can solve operation management problems and has wide use in multimedia and wireless networking [53].

The interior point algorithm (IPA) is a local search algorithm that converges rapidly and efficiently. Some problems that IPA solves are predictive control of symmetric model [54], semidefinite programming [55], linear and conic optimization [56], sum-of-squares optimization [57], etc.

3 Performance Measures

Mathematical forms of the performance measures the root mean square error (RMSE), the mean absolute deviation (MAD), and the Theil's inequality coefficient (TIC) are presented in this section.

$$\begin{bmatrix} RMSE_P \\ RMSE_Q \end{bmatrix} = \begin{bmatrix} \sqrt{\frac{1}{N}\sum_{j=1}^{N}(P_j - \hat{P}_j)^2} \\ \sqrt{\frac{1}{N}\sum_{j=1}^{N}(Q_j - \hat{Q}_j)^2} \end{bmatrix} \tag{12}$$

Table 1: Pseudocode of GAIPA to determine the weights of the GNN

Genetic Algorithm **Inputs:** Number of chromosomes that equal to the weights of GNN: $A = [A_P, A_Q]$ for $A_P = [\theta_P, \lambda_P, \gamma_P]$ and $A_Q = [\theta_Q, \lambda_Q, \gamma_Q]$ where $\theta_{\mathbf{P}} = [\theta_{P,1}, \theta_{P,2}, \cdots, \theta_{P,m}]$, $\lambda_{\mathbf{P}} = [\lambda_{P,1}, \lambda_{P,2}, \cdots, \lambda_{P,m}]$, $\gamma_{\mathbf{P}} = [\gamma_{P,1}, \gamma_{P,2}, \cdots, \gamma_{P,m}]$, $\theta_{\mathbf{Q}} = [\theta_{Q,1}, \theta_{Q,2}, \cdots, \theta_{Q,m}]$, $\lambda_{\mathbf{Q}} = [\lambda_{Q,1}, \lambda_{Q,2}, \cdots, \lambda_{Q,m}]$, $\gamma_{\mathbf{Q}} = [\gamma_{Q,1}, \gamma_{Q,2}, \cdots, \gamma_{Q,m}]$. **Output:** The best optimized weights for GNN by using GA, A_{best} **Initialization** Population and constraints: Define constraints and set initial population by real bounded entries inside constraints. **Termination** Set stopping criteria as stall generation = 100, function tolerance = 10^{-20}, constraints tolerance = 10^{-20}. **Reproduction** Use @selectionuniform, @crossoverheuristic, and @mutationadaptivefeasible in selection, crossover and mutations respectively to create new population. **Save** Store generation, function count, error function value and A_{best}. **End genetic algorithm**
Interior point algorithm start **Input** The initial weights optimized by GA, A_{best} **Output** Best weights optimized by GAIPA, A_{GAIPA} **Initialization** Define constraints and set initial population A_{best} **Termination** Set stopping criteria as @maxiteration = 20000, @maxfunevaluations = 100000, function tolerance = 10^{-20}, constraints tolerance = 10^{-20} and X tolerance = 10^{-20}. **Save** Store generation, function count, error function value and A_{GAIPA}. **End interior point algorithm**

$$\begin{bmatrix} MAD_P \\ MAD_Q \end{bmatrix} = \begin{bmatrix} \frac{1}{N}\sum_{j=1}^{N} |(P_j - \hat{P}_j)| \\ \frac{1}{N}\sum_{j=1}^{N} |(Q_j - \hat{Q}_j)| \end{bmatrix} \tag{13}$$

$$\begin{bmatrix} TIC_P \\ TIC_Q \end{bmatrix} = \begin{bmatrix} \frac{\sqrt{\frac{1}{N}\sum_{j=1}^{N}(P_j - \hat{P}_j)^2}}{\sqrt{\frac{1}{N}\sum_{j=1}^{N} P_j^2} + \sqrt{\frac{1}{N}\sum_{j=1}^{N} \hat{P}_j^2}} \\ \frac{\sqrt{\frac{1}{N}\sum_{j=1}^{N}(Q_j - \hat{Q}_j)^2}}{\sqrt{\frac{1}{N}\sum_{j=1}^{N} Q_j^2} + \sqrt{\frac{1}{N}\sum_{j=1}^{N} \hat{Q}_j^2}} \end{bmatrix} \tag{14}$$

where N denotes the number of grid points. In the case of perfect modeling, the value of RMSE, MAD, and TIC will be 0.

4 Results and Simulations

Simulations results of GNN-GAIPA for solving fractional ENSO model are presented here. The obtained results are compared with exact solution and FEM method, graphically and numerically. Two cases of the ENSO model are discussed here, one for integer order and the other for fractional order. Case 1 considered for integer order with parameters $a = 1$, $b = 0$, $c = 0.1$, $d = 1$, $e = 1$, and case 2 considered for fractional order $r = 0.85$ and parameters $a = 1$, $b = 1$, $c = 0.1$, $d = 1$, $e = 1$. The mathematical form of both cases is represented as follows
Case 1

$$\begin{cases} DP = P - 0.1P^3 \\ DQ = -P - Q \end{cases} \tag{15}$$

Case 2

$$\begin{cases} {}_0D_t^{0.85}P = P + Q - 0.1P^3 \\ {}_0D_t^{0.85}Q = -P - Q \end{cases} \tag{16}$$

Figure 1 shows the optimal weights for both cases for 10 neurons. These plots represents the values of θ, λ, and γ. Figure 1 drown for best weight vectors which are shown in Eq. (17 & 18). Figure 2 compares the approximated solution to the exact solution and FEM solution. The proposed result overlaps with the exact solution and FEM solution, showing the efficiency of the proposed method.
The best absolute errors (AE) are presented in figure (3) calculated for 20 independent trials for both cases. The best absolute error lie in $10^{-6} - 10^{-5}$ for case 1 and $10^{-3} - 10^{-2}$ for case 2. These absolute errors indicate the proposed GNN along with GAIPA effectively solves the ENSO model.
The RMSE, MAD, and TIC for both cases of the ENSO model are plotted in figure (4). The performance measures RMSE, MAD, and TIC for case 1 lie between $10^{-6} - 10^{-5}$, $10^{-6} - 10^{-5}$, and $10^{-7} - 10^{-5}$ respectively, and for case 2, the performance measures lie between $10^{-3} - 10^{-2}$, $10^{-3} - 10^{-2}$, and $10^{-3} - 10^{-2}$ respectively.
Statical performance for RMSE, MAD, and TIC using the histogram and boxplots are presented in figure (5-7).
The tabular comparison was also made in tables (2 & 3) for the proposed method with exact and FEM solution. Table 2 is made for the classical order case, where the obtained solution is compared with the exact solution, and Table 3 is made for the fractional order case, where the obtained solution is compared with the fractional Euler's method.
The solution of the ENSO model using the proposed method shows that the value of P (sea surface temperature) increases concerning time and Q (thermo-cline depth anomaly) decreases concerning time in the time interval $[0, 1]$.

$$\begin{bmatrix} \hat{P}_{C-1} \\ \hat{Q}_{C-1} \end{bmatrix} = \begin{bmatrix} 0.2939\left(2tan^{-1}e^{(0.3293x+2.2331)} - \frac{\pi}{2}\right) + 0.0036\left(2tan^{-1}e^{(-0.3587x-1.5049)} - \frac{\pi}{2}\right) + \\ \cdots - 0.2041\left(2tan^{-1}e^{(1.1775x+1.9143)} - \frac{\pi}{2}\right) \\ -0.3452\left(2tan^{-1}e^{(0.7770x+0.3393)} - \frac{\pi}{2}\right) + 0.1293\left(2tan^{-1}e^{(1.6931x+0.7418)} - \frac{\pi}{2}\right) + \\ \cdots - 0.1274\left(2tan^{-1}e^{(0.8965x+0.5762)} - \frac{\pi}{2}\right) \end{bmatrix} \tag{17}$$

$$\begin{bmatrix} \hat{P}_{C-2} \\ \hat{Q}_{C-2} \end{bmatrix} = \begin{bmatrix} 0.1206\left(2tan^{-1}e^{(-0.8466x+0.1391)} - \frac{\pi}{2}\right) - 0.9109\left(2tan^{-1}e^{(-2.1315x+1.2730)} - \frac{\pi}{2}\right) + \\ \cdots + 1.1796\left(2tan^{-1}e^{(-0.4855x-0.7389)} - \frac{\pi}{2}\right) \\ 1.1055\left(2tan^{-1}e^{(-4.8031x-2.0155)} - \frac{\pi}{2}\right) + 0.4167\left(2tan^{-1}e^{(-0.2833x-3.0836)} - \frac{\pi}{2}\right) + \\ \cdots - 0.7407\left(2tan^{-1}e^{(0.5212x+1.1957)} - \frac{\pi}{2}\right) \end{bmatrix} \tag{18}$$

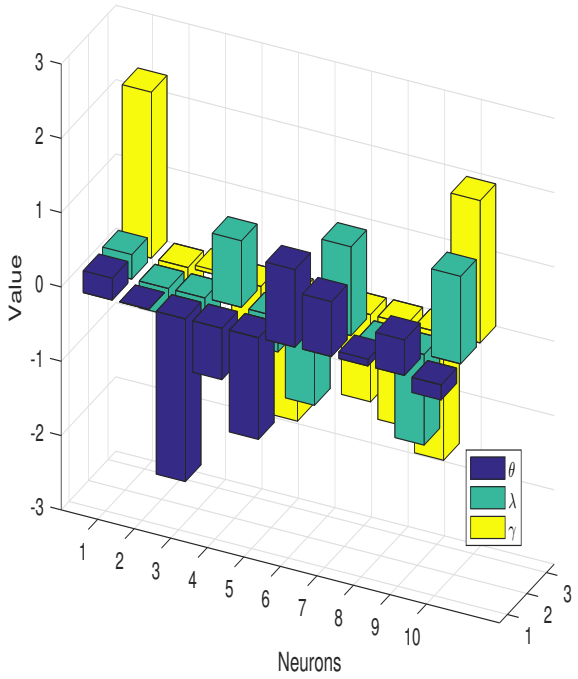

(a) Case 1: weights for P

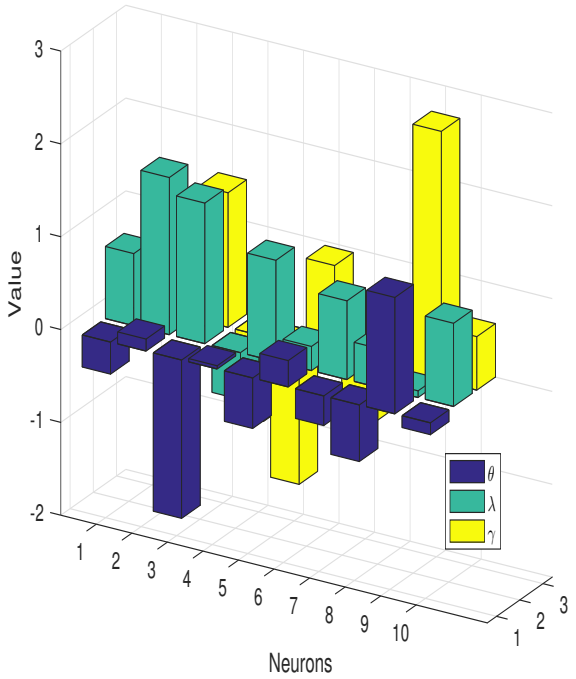

(b) Case 1: weights for Q

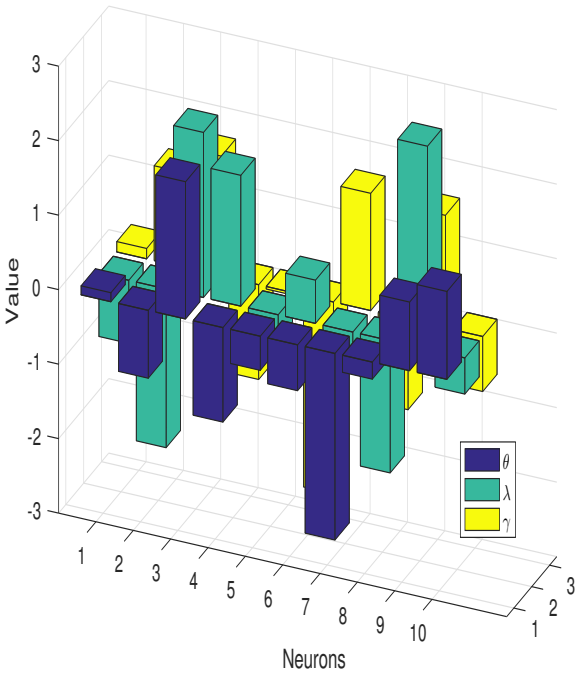

(c) Case 2: weights for P

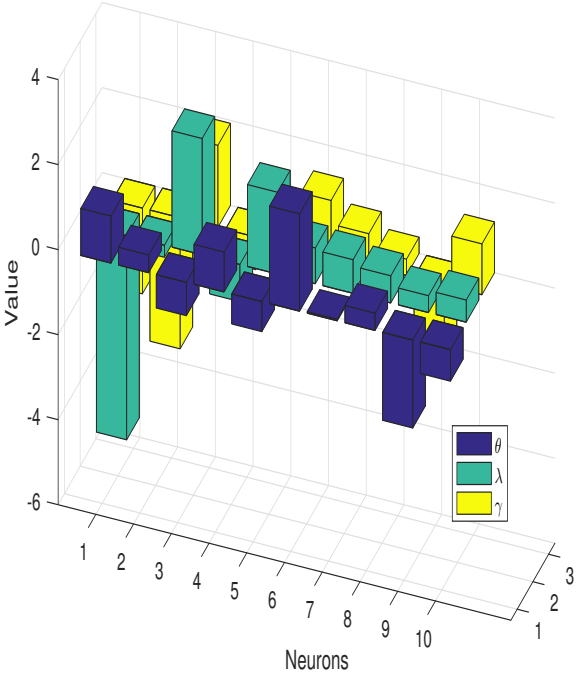

(d) Case 2: weights for Q

Fig. 1: Best weights for the proposed network

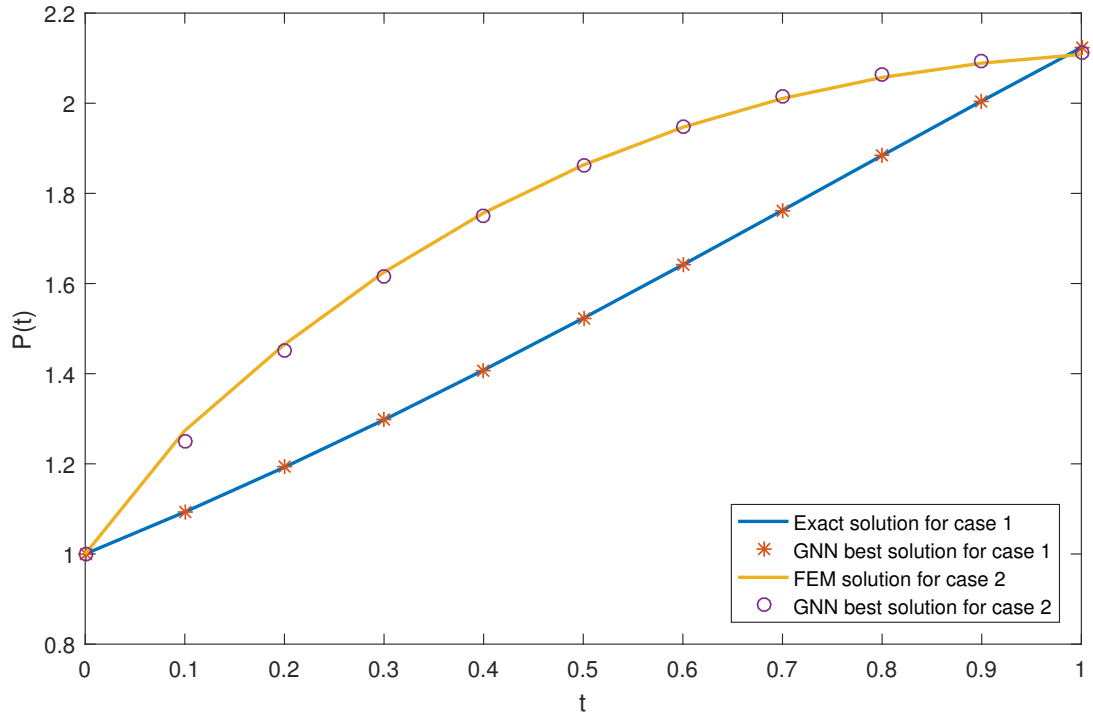

(a) Comparison of the obtained solution with exact and FEM solution for P(t)

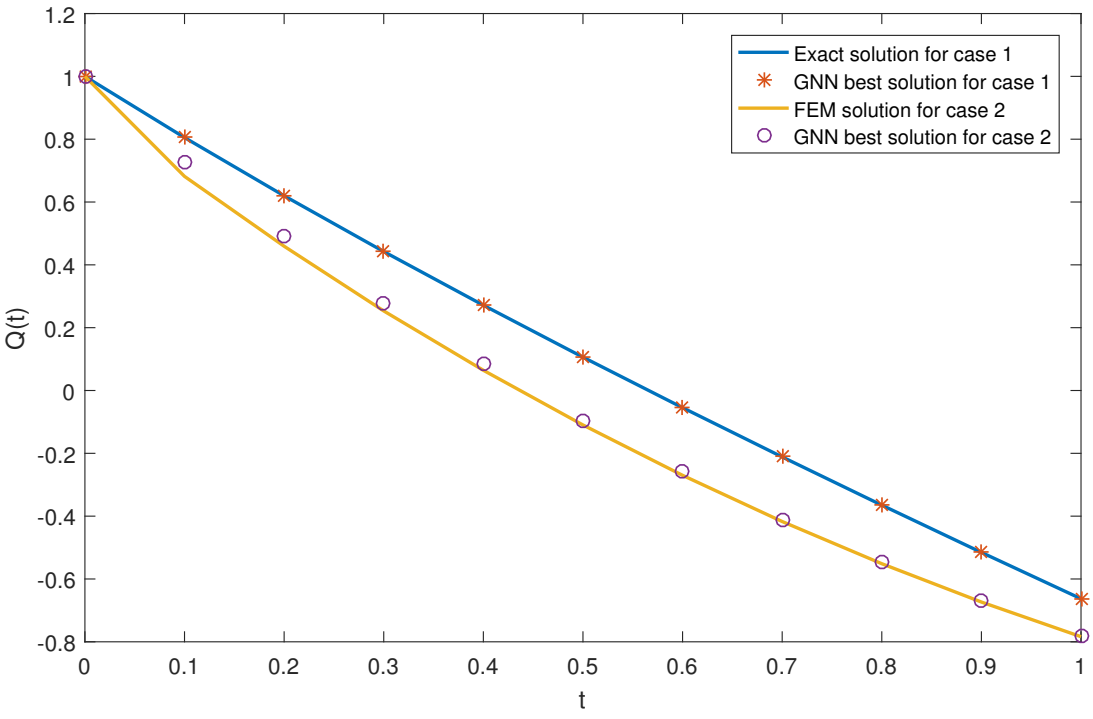

(b) Comparison of the obtained solution with exact and FEM solution for Q(t)

Fig. 2: Comparison of proposed result with exact and FEM solution

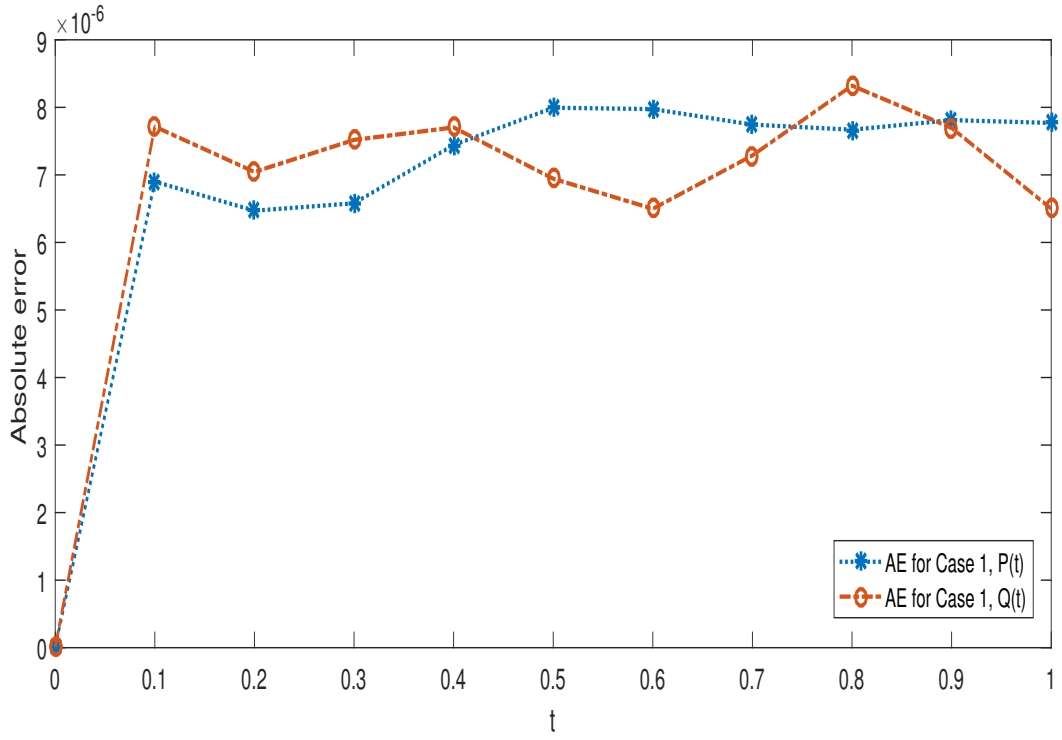

(a) Absolute errors for case 1

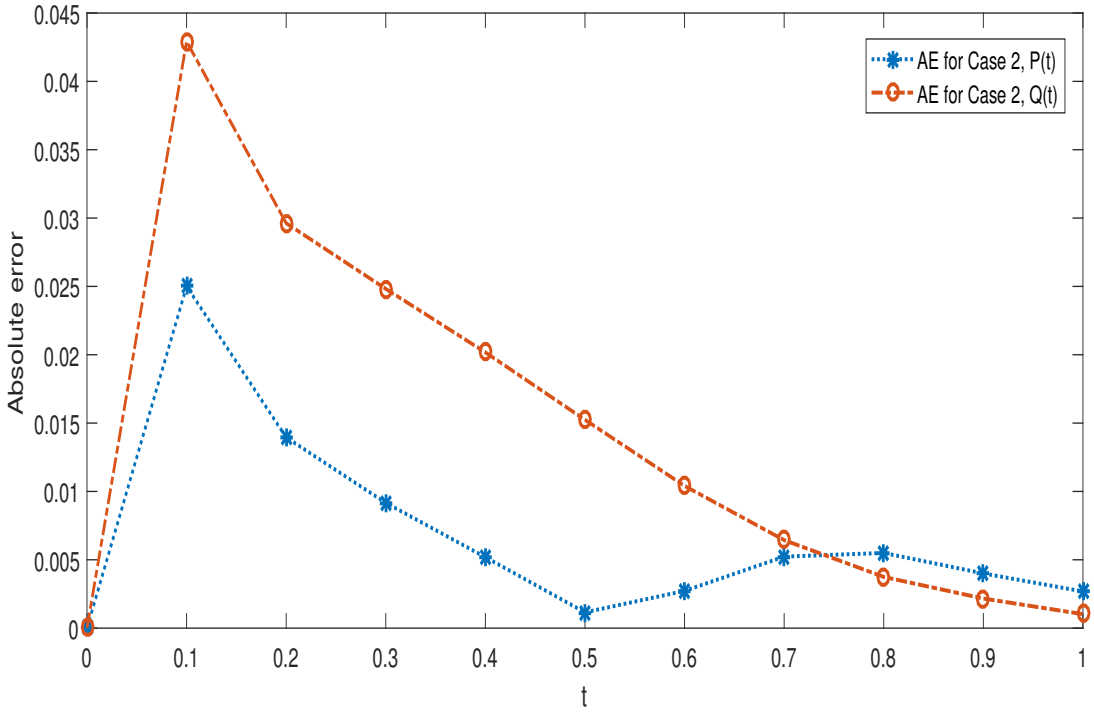

(b) Absolute errors for case 2

Fig. 3: Absolute Error

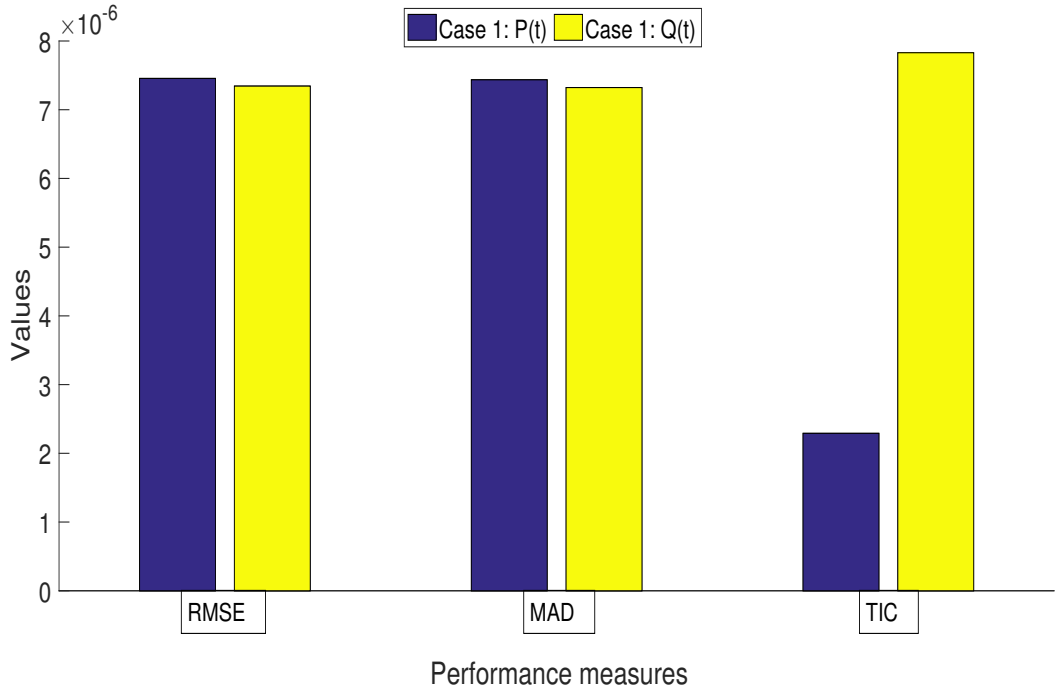

(a) Performance measures for case 1

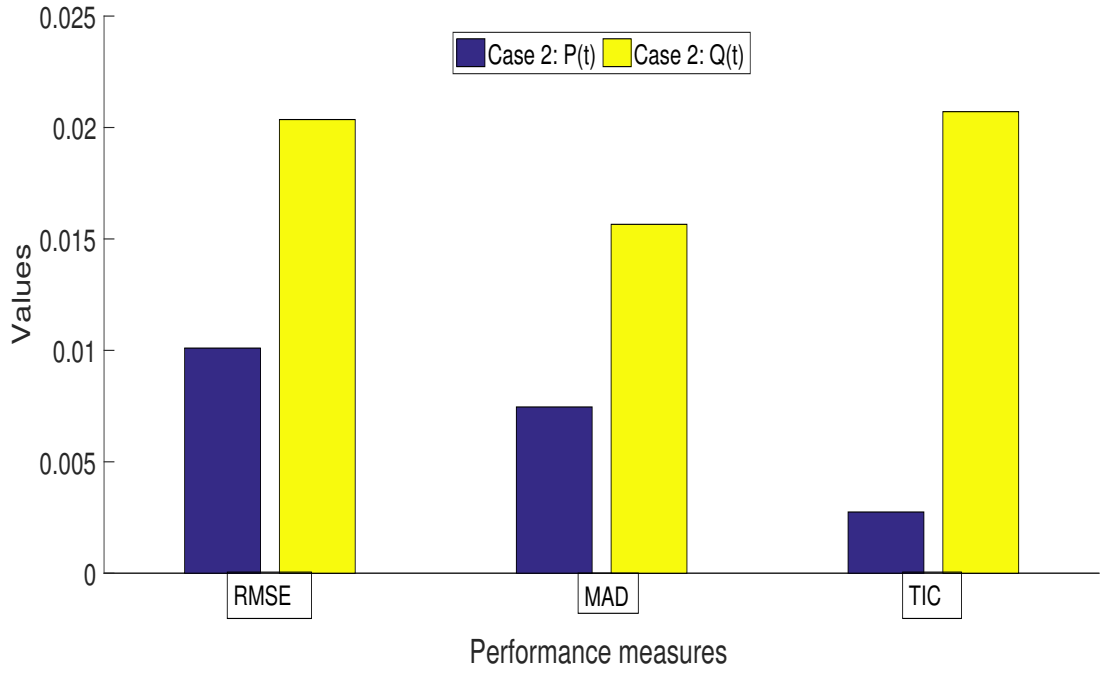

(b) Performance measures for case 2

Fig. 4: Performance measures

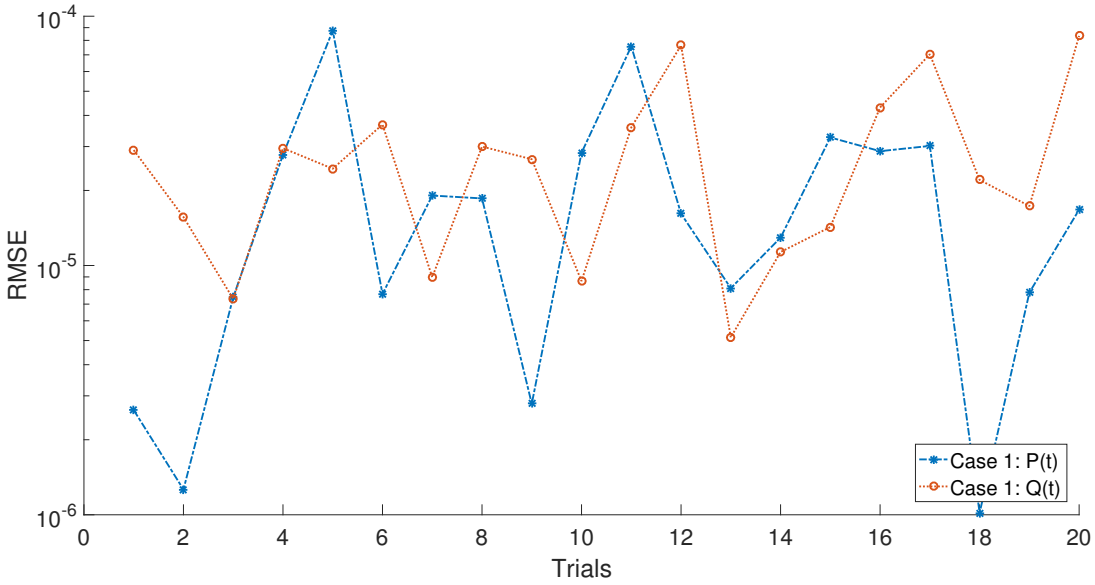

(a) Case 1 RMSE for all 20 Trials

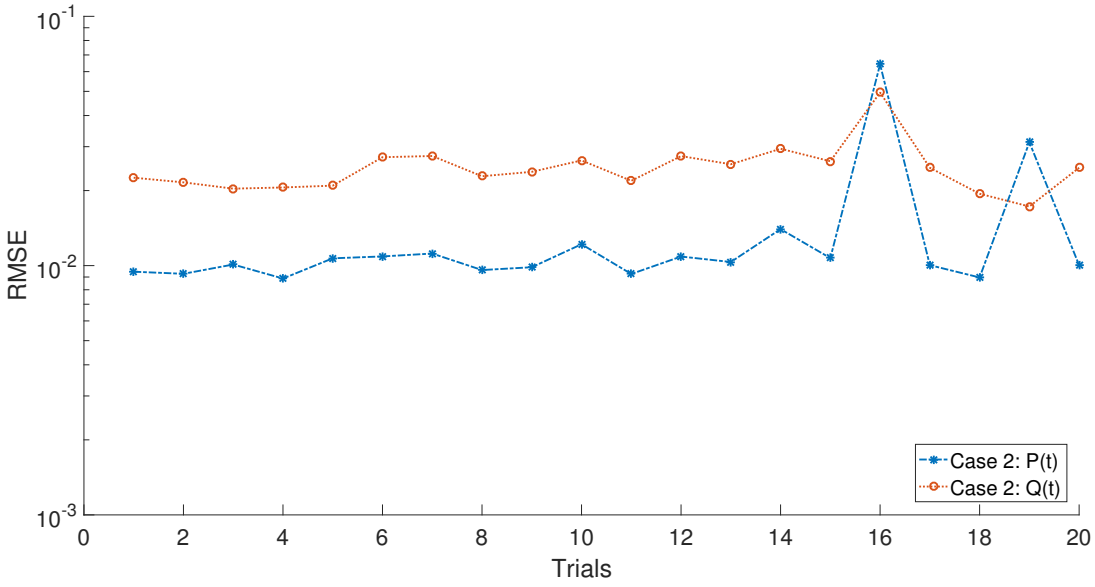

(b) Case 2 RMSE for all 20 Trials

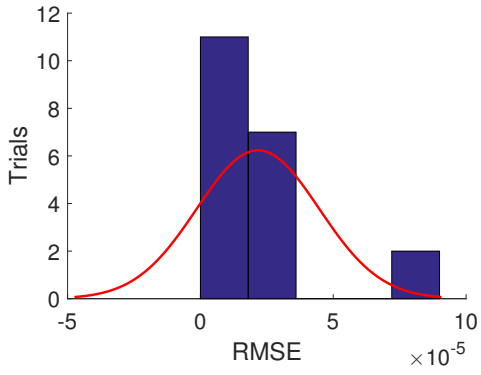

(c) Case 1 P(t) histogram

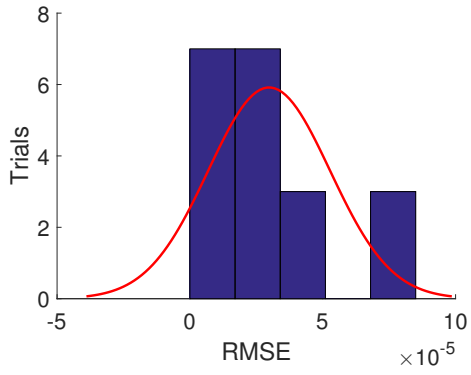

(d) Case 1 Q(t) histogram

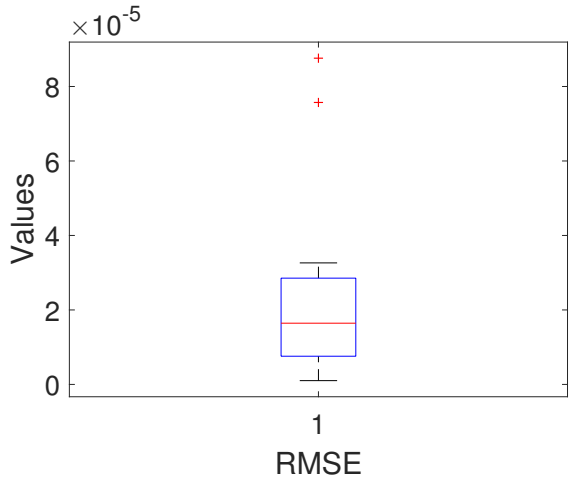

(e) Case 1 P(t) boxplot

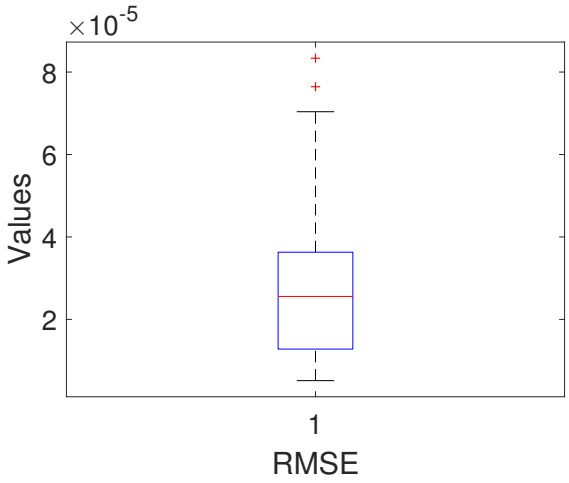

(f) Case 1 Q(t) boxplot

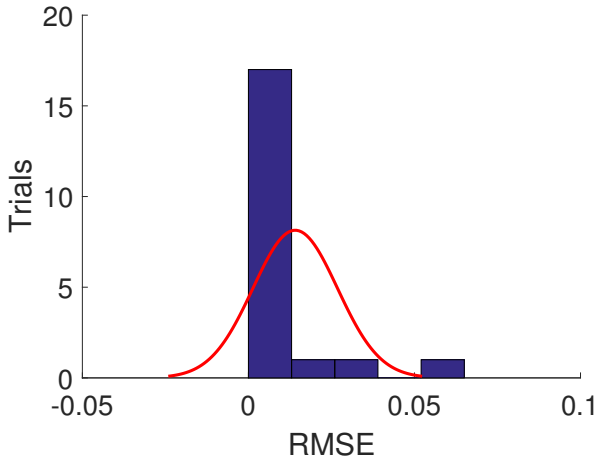

(g) Case 2 P(t) histogram

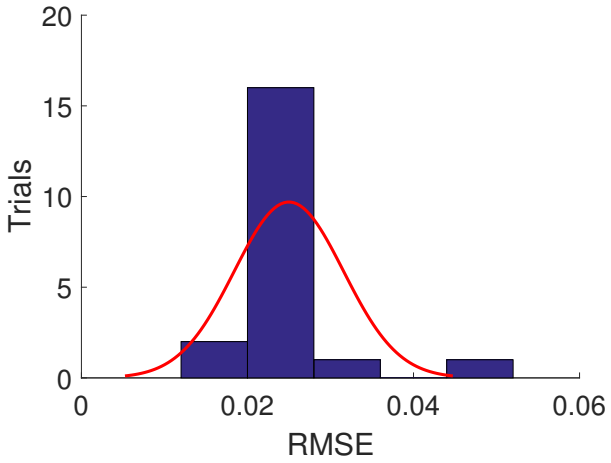

(h) Case 2 Q(t) histogram

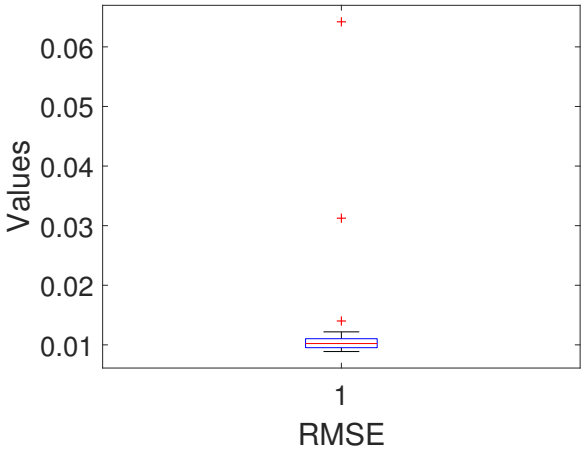

(i) Case 2 P(t) boxplot

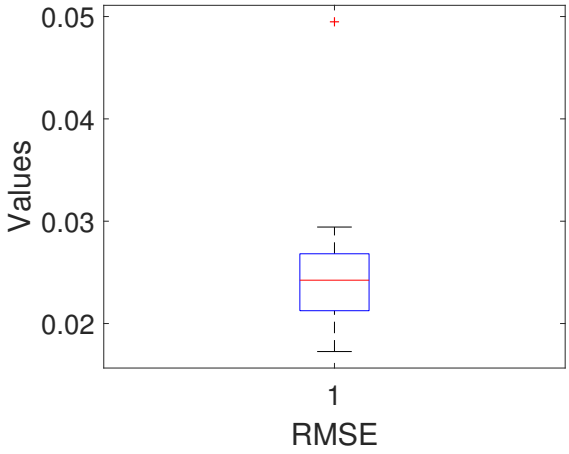

(j) Case 2 Q(t) boxplot

Fig. 5: RMSE representation for ENSO model through GNN-GAIPA

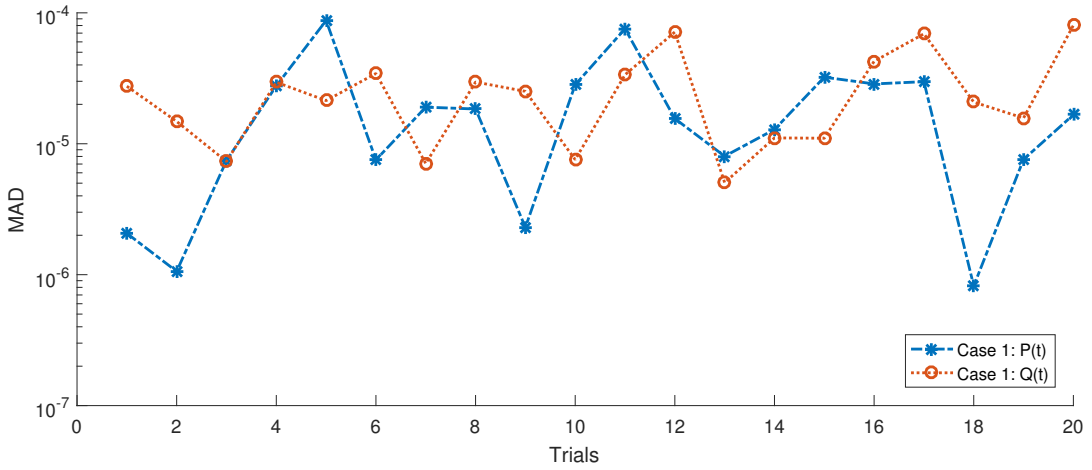

(a) Case 1 MAD for all 20 Trials

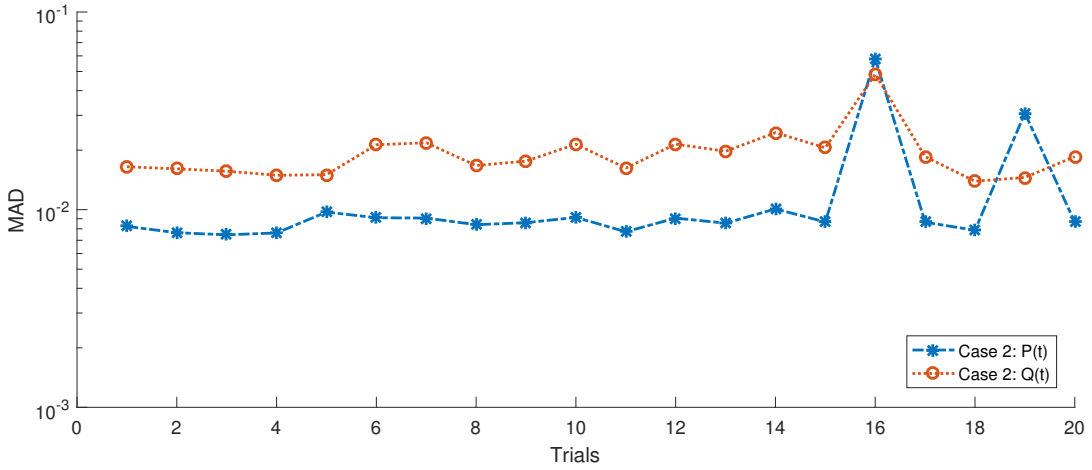

(b) Case 2 MAD for all 20 Trials

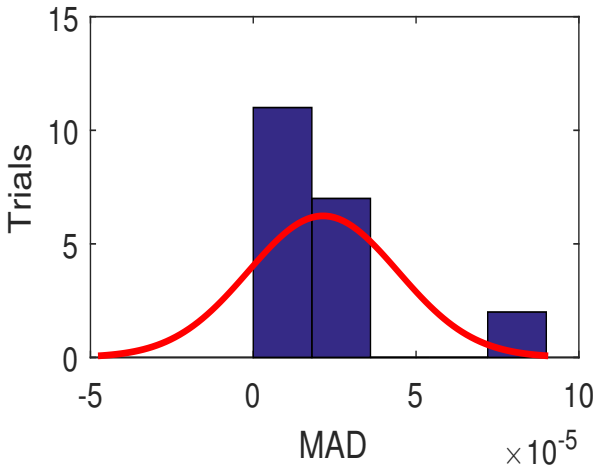

(c) Case 1 P(t) histogram

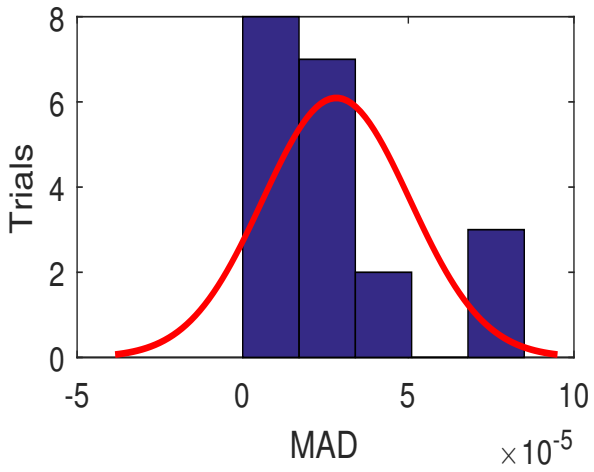

(d) Case 1 Q(t) histogram

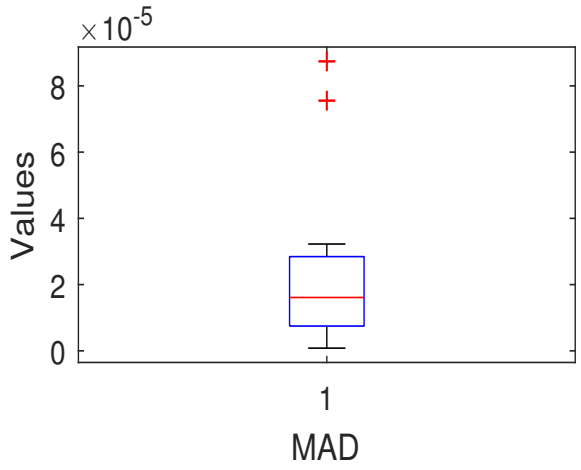

(e) Case 1 P(t) boxplot

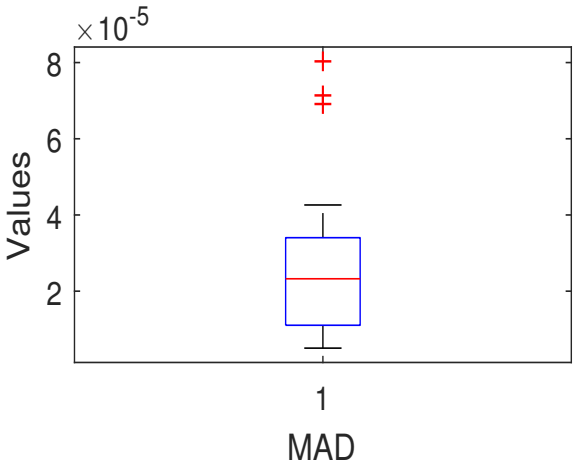

(f) Case 1 Q(t) boxplot

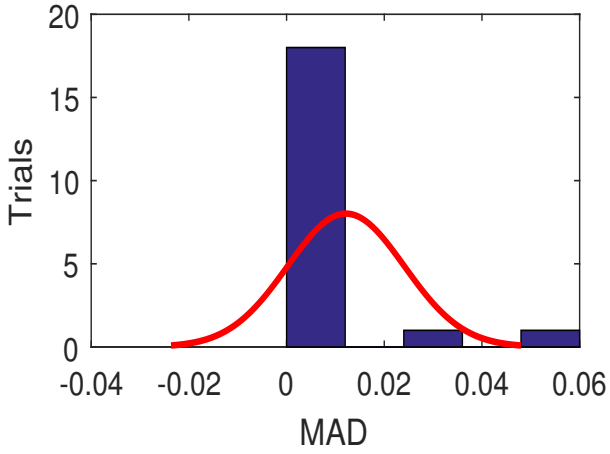

(g) Case 2 P(t) histogram

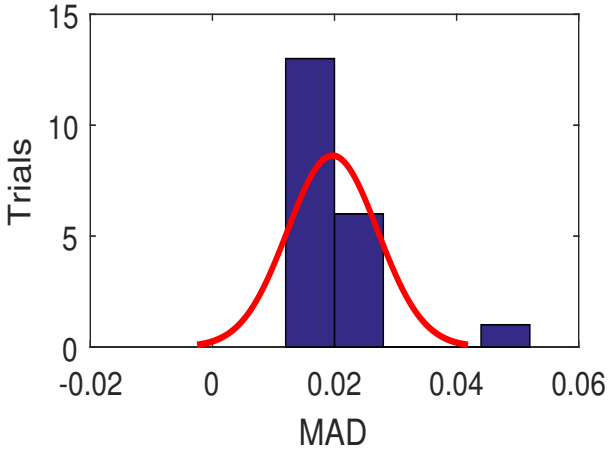

(h) Case 2 Q(t) histogram

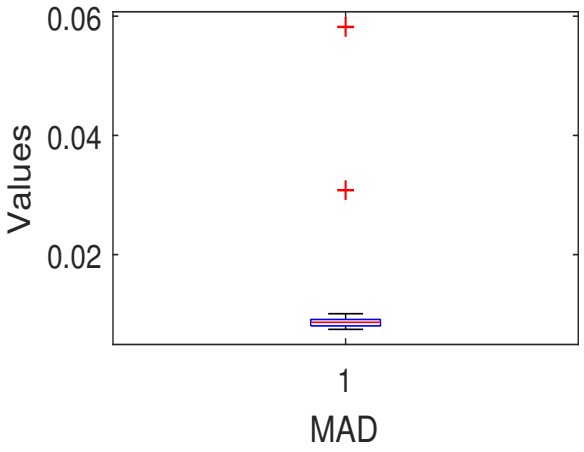

(i) Case 2 P(t) boxplot

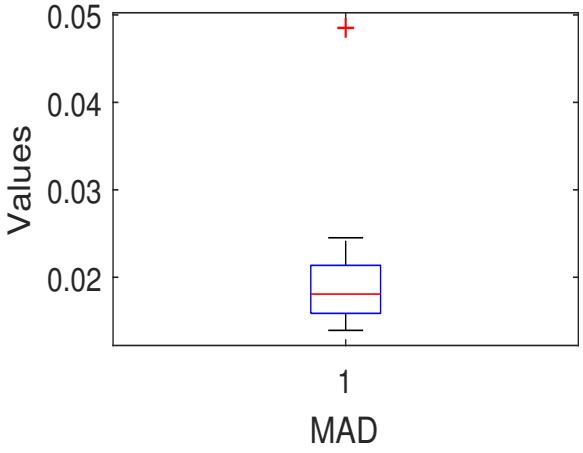

(j) Case 2 Q(t) boxplot

Fig. 6: MAD representation for ENSO model through GNN-GAIPA

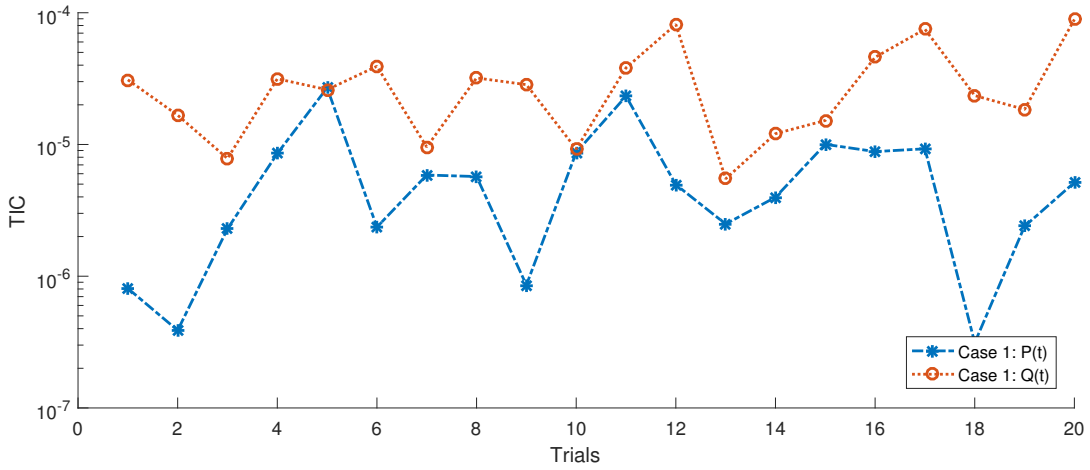

(a) Case 1 TIC for all 20 Trials

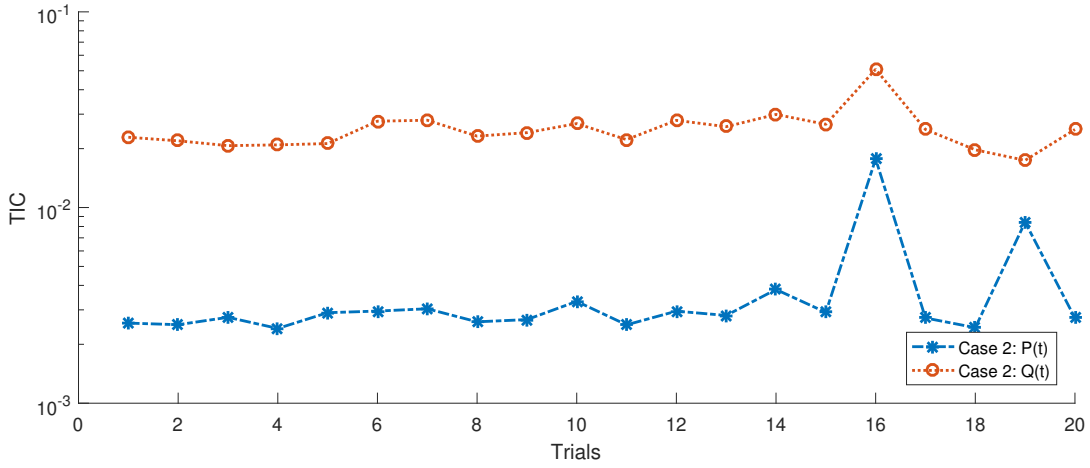

(b) Case 2 TIC for all 20 Trials

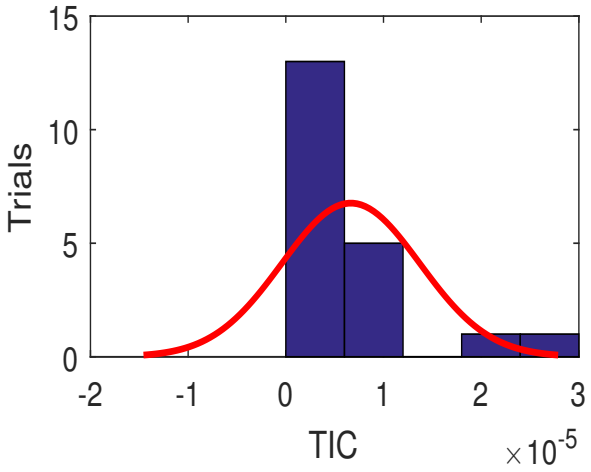

(c) Case 1 P(t) histogram

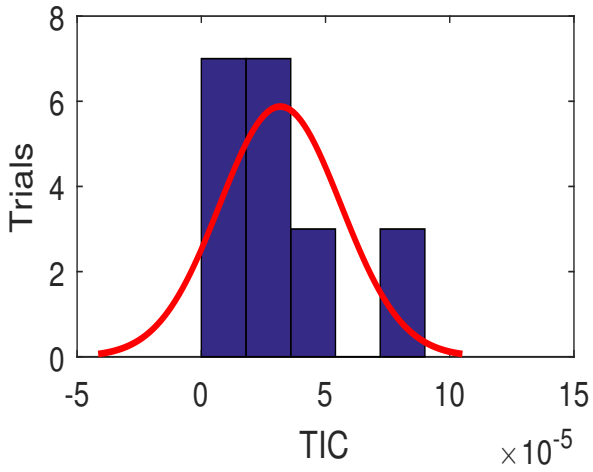

(d) Case 1 Q(t) histogram

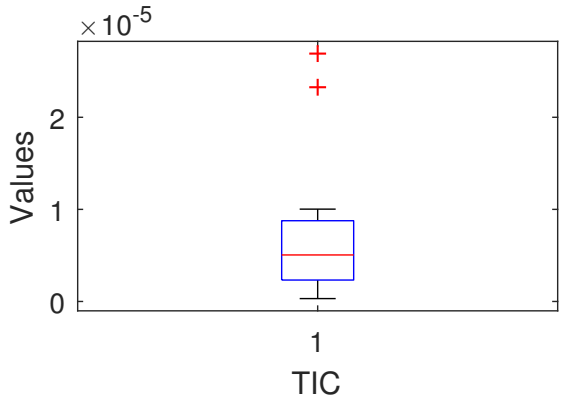

(e) Case 1 P(t) boxplot

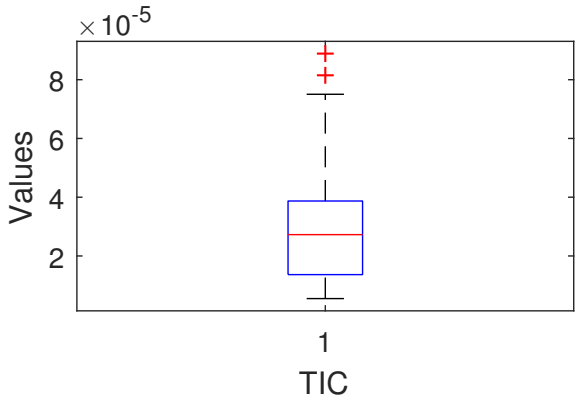

(f) Case 1 Q(t) boxplot

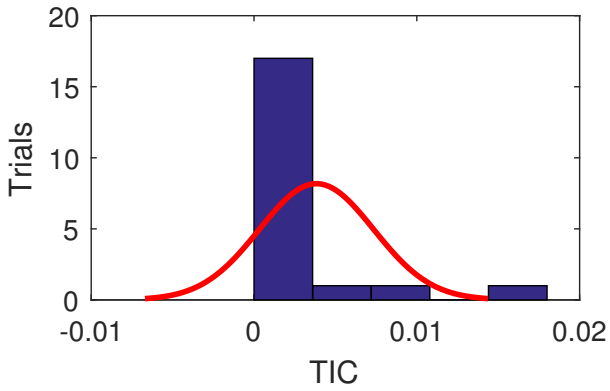

(g) Case 2 P(t) histogram

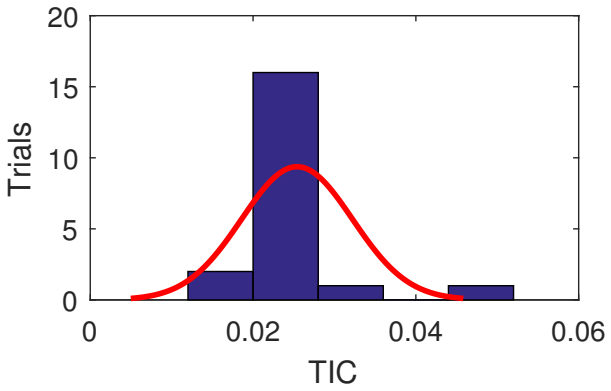

(h) Case 2 Q(t) histogram

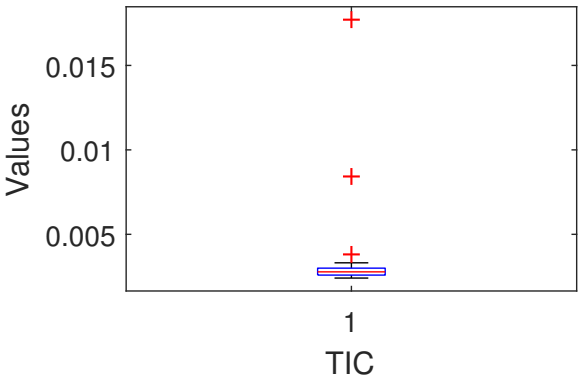

(i) Case 2 P(t) boxplot

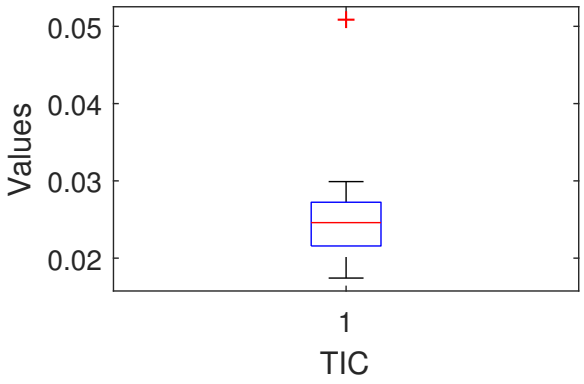

(j) Case 2 Q(t) boxplot

Fig. 7: TIC representation for ENSO model through GNN-GAIPA

5 Conclusions

The present work is related to construct a Gudermannian neural network algorithm for the fractional El Niño Southern Oscillation model. Two different cases one for classical order and one for fractional order have been solved by using the designed GNN algorithm and optimized by the hybridization of global search algorithm, the ganatic algorithm and local search algorithm, the interior point algorithm i.e. GNN-GAIPA. The designed GNN-GAIPA is viably implemented on

Table 2: Comparison of proposed solution with exact solution for case 1

t	Case 1 P(t)		Case 1 Q(t)	
	Proposed	Exact	Proposed	Exact
0.0	1	1	1	1
0.1	1.0931	1.0931	0.8052	0.8052
0.2	1.1924	1.1924	0.6198	0.6198
0.3	1.2976	1.2976	0.4423	0.4423
0.4	1.4080	1.4080	0.2714	0.2714
0.5	1.5230	1.5231	0.1061	0.1061
0.6	1.6416	1.6416	-0.0547	-0.0547
0.7	1.7624	1.7624	-0.2115	-0.2115
0.8	1.8841	1.8841	-0.3650	-0.3650
0.9	2.0049	2.0049	-0.5154	-0.5154
1.0	2.1233	2.1233	-0.6629	-0.6629

Table 3: Comparison of the proposed solution with FEM solution for case 2

t	Case 2 P(t)		Case 2 Q(t)	
	Proposed	FEM solution	Proposed	FEM solution
0.0	1	1	1	1
0.1	1.2486	1.2736	0.7246	0.6816
0.2	1.4508	1.4647	0.4889	0.4593
0.3	1.6160	1.6252	0.2781	0.2532
0.4	1.7515	1.7567	0.0846	0.0644
0.5	1.8618	1.8629	-0.0945	-0.1098
0.6	1.9494	1.9467	-0.2597	-0.2701
0.7	2.0158	2.0106	-0.4107	-0.4171
0.8	2.0627	2.0572	-0.5476	-0.5514
0.9	2.0930	2.0890	-0.6712	-0.6734
1.0	2.1108	2.1081	-0.7827	-0.7837

both classical and fractional ENSO model to authenticate the stability, convergence and robustness. The outcomes of the proposed scheme have been compaired with exact and FEM solution with matching 5 to 6 decimal places of accuracy in case 1 and 2 to 3 places in case 2. Statistical performance measures for 20 independent trials for both the cases provide the precise solutions.

References

[1] C. A. Varotsos, A. P. Cracknell and M. N. Efstathiou, The global signature of the El Niño/La Niña Southern Oscillation. International Journal of Remote Sensing, 39(18), 5965–5977 (2018). https://doi.org/10.1080/01431161.2018.1465617
[2] C. F. Ropelewski and M. S. Halpert, Global and regional scale precipitation patterns associated with the El Niño/Southern Oscillation. Mon. Weather Rev. 115, 1606–1626 (1987).
[3] J. M. Arblaster and L. V. Alexander, The impact of the El Niño-Southern Oscillation on maximum temperature extremes, Geophys. Res. Lett., 39, L20702 (2012). doi:10.1029/2012GL053409.
[4] M. J. McPhaden, A. Santoso and W. Cai, (eds) El Niño Southern Oscillation in a Changing Climate Vol. 253 (Wiley, 2020).
[5] K. E. Trenberth, The definition of el nino. Bulletin of the American Meteorological Society, 78(12), 2771-2778 (1997).
[6] M. J. McPhaden, S. E. Zebiak and M. H. Glantz, ENSO as an integrating concept in earth science. science, 314(5806), 1740-1745 (2006).
[7] S. G. Philander, El Niño, La Niña, and the southern oscillation. International geophysics series, 46, X-289 (1989).
[8] M. H. Glantz, Currents of change: impacts of El Niño and La Niña on climate and society. Cambridge University Press (2001).
[9] K. AchutaRao and K. Sperber, Simulation of the El Niño Southern Oscillation: Results from the Coupled Model Intercomparison Project. Climate Dynamics 19, 191–209 (2002). https://doi.org/10.1007/s00382-001-0221-9
[10] C. Wang, A Unified Oscillator Model for the El Niño–Southern Oscillation. J. Climate, 14, 98–115 (2001).
[11] Y. Wei, J. Zhang, L. Bai and Y. Wang, Connectedness among El Niño-Southern Oscillation, carbon emission allowance, crude oil and renewable energy stock markets: Time- and frequency-domain evidence based on TVP-VAR model, Renewable Energy, Volume 202, Pages 289-309, ISSN 0960-1481 (2023). https://doi.org/10.1016/j.renene.2022.11.098.

[12] N. Maher, R. C. J. Wills, P. Dinezio, J. Klavans, S. Milinski, S. C. Sanchez, S. Stevenson, M. F. Stuecker and X. Wu, The future of the El Niño-Southern Oscillation: using large ensembles to illuminate time-varying responses and inter-model differences. Earth System Dynamics, 14(2), 413-431. https://doi.org/10.5194/esd-14-413-2023 (2023).
[13] K. Baier, M. Duetsch, M. Mayer, L. Bakels, L. Haimberger and A. Stohl, The role of atmospheric transport for El Niño-Southern Oscillation teleconnections. Geophysical Research Letters, 49, e2022GL100906 (2022). https://doi. org/10.1029/2022GL100906
[14] Y. You, J. Liu, Y. Zhang, H. E. Beck, X. Gu and D. Kong, Impacts of El Niño–Southern Oscillation on Global Runoff: Characteristic Signatures and Potential Mechanisms. Hydrological Processes (2021). doi:10.1002/hyp.14367
[15] I. Podlubny, Fractional differential equations: an introduction to fractional derivatives, fractional differential equations, to methods of their solution and some of their applications, elsevier (1998).
[16] A. A. Kilbas, H. M. Srivastava and J. J. Trujillo, Theory and applications of fractional differential equations (Vol. 204), elsevier (2006).
[17] K. Oldham, and J. Spanier, The fractional calculus theory and applications of differentiation and integration to arbitrary order, Elsevier (1974).
[18] K. S. Miller and B. Ross, An introduction to the fractional calculus and fractional differential equations, Wiley (1993).
[19] F. Mainardi, Fractional calculus and waves in linear viscoelasticity: an introduction to mathematical models. World Scientific (2022).
[20] M.A. Pinto Carla and R.M. Carvalho Ana, A latency fractional order model for HIV dynamics, Journal of Computational and Applied Mathematics, Volume 312, 2017, Pages 240-256, ISSN 0377-0427 (2017). https://doi.org/10.1016/j.cam.2016.05.019.
[21] G. A. Anastassiou, A strong fractional calculus theory for Banach space valued functions. Nonlinear Functional Analysis and Applications, 22(3), 495 (2017).
[22] J. Losada and J. Nieto, Properties of a new fractional derivative without singular Kernel. Prog Fract Differ Appl. 1. 87-92 (2015). 10.12785/pfda/010202.
[23] S. Kumar, R. Kumar, C. Cattani and B. Samet, Chaotic behaviour of fractional predator-prey dynamical system, Chaos, Solitons & Fractals, Volume 135, (2020), 109811, ISSN 0960-0779 (2020). https://doi.org/10.1016/j.chaos.2020.109811.
[24] H. Jafari and V. D. Gejji, Solving a system of nonlinear fractional differential equations using Adomian decomposition, Journal of Computational and Applied Mathematics, Volume 196, Issue 2, 2006, Pages 644-651, ISSN 0377-0427 (2006). https://doi.org/10.1016/j.cam.2005.10.017.
[25] R. Jan, E. Hinçal, K. Hosseini, N. N. A. Razak, T. Abdeljawad and M. S. Osman, Fractional view analysis of the impact of vaccination on the dynamics of a viral infection, Alexandria Engineering Journal, Volume 102, Pages 36-48, ISSN 1110-0168 (2024). https://doi.org/10.1016/j.aej.2024.05.080.
[26] R. Garrappa, E. Kaslik and M. Popolizio, Evaluation of Fractional Integrals and Derivatives of Elementary Functions: Overview and Tutorial. Mathematics 2019, 7, 407 (2019). https://doi.org/10.3390/math7050407
[27] S. Rezapour, S. Etemad and H. Mohammadi, A mathematical analysis of a system of Caputo–Fabrizio fractional differential equations for the anthrax disease model in animals. Advances in Difference Equations, 2020(1), 481.
[28] M. Cai, C. Li, Numerical Approaches to Fractional Integrals and Derivatives: A Review. Mathematics. (2020); 8(1):43. https://doi.org/10.3390/math8010043
[29] D. Kumar, H. Nama, J. Singh, and J. Kumar, An Efficient Numerical Scheme for Fractional Order Mathematical Model of Cytosolic Calcium Ion in Astrocytes. Fractal Fract. (2024), 8, 184. https://doi.org/10.3390/fractalfract8040184
[30] D. Kumar, R. P. Agarwal, J. Singh, A modified numerical scheme and convergence analysis for fractional model of Lienard's equation, Journal of Computational and Applied Mathematics, Volume 339, Pages 405-413, ISSN 0377-0427 (2018). https://doi.org/10.1016/j.cam.2017.03.011.
[31] S. Kumar, D. Kumar and J. Singh, Numerical computation of fractional Black–Scholes equation arising in financial market, Egyptian Journal of Basic and Applied Sciences, Volume 1, Issues 3–4, Pages 177-183, ISSN 2314-808X (2014). https://doi.org/10.1016/j.ejbas.2014.10.003.
[32] J. Singh, D. Kumar, M. A. Qurashi and D. Baleanu, A new fractional model for giving up smoking dynamics. Advances in Difference Equations, 2017(1), 88.
[33] J. Singh, D. Kumar and J. J. Nieto, Analysis of an El Nino-Southern Oscillation model with a new fractional derivative. Chaos, Solitons & Fractals, 99, 109-115 (2017).
[34] Y. Zhang, P. Li, C. Xu, X. Peng and R. Qiao, Investigating the Effects of a Fractional Operator on the Evolution of the ENSO Model: Bifurcations, Stability and Numerical Analysis. Fractal and Fractional. 7. 602, (2023). 10.3390/fractalfract7080602.
[35] X. Li and Y. Li, The El Niño Southern Oscillation Recharge Oscillator with the Stochastic Forcing of Long-Term Memory. Fractal and Fractional. 8(2):121 (2024). https://doi.org/10.3390/fractalfract8020121
[36] Y. Zeng, The Laplace-Adomian-Pade Technique for the ENSO Model. Mathematical Problems in Engineering, 2013, 1–4 (2013). doi:10.1155/2013/954857
[37] J. Mo and W. Lin, Generalized variation iteration solution of an atmosphere-ocean oscillator model for global climate. J Syst Sci Complex 24, 271–276 (2011). https://doi.org/10.1007/s11424-011-7153-1
[38] J. F. Gómez-Aguilar, Multiple attractors and periodicity on the Vallis model for El Niño/La Niña-Southern oscillation model. Journal of Atmospheric and Solar-Terrestrial Physics, 105172 (2019). doi:10.1016/j.jastp.2019.105172
[39] S. Mall and S. Chakraverty, Application of Legendre Neural Network for solving ordinary differential equations, Applied Soft Computing, Volume 43, Pages 347-356, ISSN 1568-4946 (2016). https://doi.org/10.1016/j.asoc.2015.10.069.

[40] A. Jafarian, M. Mokhtarpour and D. Baleanu, Artificial neural network approach for a class of fractional ordinary differential equation. Neural Computing and Applications, 28(4), 765–773 (2016). doi:10.1007/s00521-015-2104-8
[41] Z. Sabir, M. A. Z. Raja, J. L. G. Guirao and M. Shoaib, A novel design of fractional Meyer wavelet neural networks with application to the nonlinear singular fractional Lane-Emden systems, Alexandria Engineering Journal, Volume 60, Issue 2, Pages 2641-2659, ISSN 1110-0168 (2021). https://doi.org/10.1016/j.aej.2021.01.004.
[42] Z. Sabir, M. Umar, H. A. Wahab, S. A. Bhat and C. Unlu, Heuristic computing performances based Gudermannian neural network to solve the eye surgery corneal model, Applied Soft Computing, Volume 157, 111540, ISSN 1568-4946 (2024). https://doi.org/10.1016/j.asoc.2024.111540.
[43] I. Ahmad, F. Ahmad, M. A. Z. Raja, H. Ilyas, N. Anwar and Z. Azad, Intelligent computing to solve fifth-order boundary value problem arising in induction motor models. Neural Computing and Applications, 29(7), 449-466 (2018).
[44] A. H. H. Rasanan, D. Rahmati, S. Gorgin and K. Parand, A single layer fractional orthogonal neural network for solving various types of Lane–Emden equation, New Astronomy, Volume 75, 101307, ISSN 1384-1076 (2020). https://doi.org/10.1016/j.newast.2019.101307.
[45] R. Saneifard, A. Jafarian, N. Ghalami and S. M. Nia, Extended artificial neural networks approach for solving two-dimensional fractional-order Volterra-type integro-differential equations, Information Sciences, Volume 612, Pages 887-897, ISSN 0020-0255 (2022). https://doi.org/10.1016/j.ins.2022.09.017.
[46] N. A. Khan, O. I. Khalaf, C. A. Tavera Romero, M. Sulaiman and M. A. Bakar, Application of Intelligent Paradigm through Neural Networks for Numerical Solution of Multiorder Fractional Differential Equations. Computational Intelligence and Neuroscience, 2022(1), 2710576 (2021). https://doi.org/10.1155/2022/2710576
[47] M.A.Z. Raja, M.A. Manzar and R. Samar, An efficient computational intelligence approach for solving fractional order Riccati equations using ANN and SQP, Applied Mathematical Modelling, Volume 39, Issues 10–11, Pages 3075-3093, ISSN 0307-904X (2015). https://doi.org/10.1016/j.apm.2014.11.024.
[48] Yi. Zeng, The Laplace-Adomian-Pade technique for the ENSO model. Mathematical Problems in Engineering. (2013). 10.1155/2013/954857.
[49] H. Ahmed, FRACTIONAL EULER METHOD; AN EFFECTIVE TOOL FOR SOLVING FRACTIONAL DIFFERENTIAL EQUATIONS. Journal of the Egyptian Mathematical Society. 26. 38-43 (2018). 10.21608/JOEMS.2018.9460.
[50] C. Cavallaro, V. Cutello, M. Pavone and F. Zito, Machine Learning and Genetic Algorithms: A case study on image reconstruction, Knowledge-Based Systems, Volume 284, 111194, ISSN 0950-7051 (2024). https://doi.org/10.1016/j.knosys.2023.111194.
[51] Z. Li, B. Shen, H. Wan and B. Fricke, Heat exchanger circuitry optimization using an enhanced integer permutation-based genetic algorithm in low-GWP reversible heat pump applications, Applied Thermal Engineering, Volume 239, 122111, ISSN 1359-4311 (2024). https://doi.org/10.1016/j.applthermaleng.2023.122111.
[52] T. S. Delwar, A. Siddique, U. Aras and J.Y. Ryu, A Design of Adaptive Genetic Algorithm-Based Optimized Power Amplifier for 5G Applications. Circuits Syst Signal Process 43, 2–21 (2024). https://doi.org/10.1007/s00034-023-02447-7
[53] S. Katoch, S.S. Chauhan and V. Kumar, A review on genetic algorithm: past, present, and future. Multimedia Tools and Applications (2020). doi:10.1007/s11042-020-10139-6
[54] S. Panahi, A. Kashani and C. Danielson, Primal–dual interior-point algorithm for symmetric model predictive control, Automatica, Volume 155, 111157, ISSN 0005-1098, (2023). https://doi.org/10.1016/j.automatica.2023.111157.
[55] H. Jiang, T. Kathuria, Y. T. Lee, S. Padmanabhan and Z. Song, "A Faster Interior Point Method for Semidefinite Programming," 2020 IEEE 61st Annual Symposium on Foundations of Computer Science (FOCS), Durham, NC, USA, pp. 910-918 (2020). doi: 10.1109/FOCS46700.2020.00089.
[56] Q. Deng, Q. Feng, W. Gao, D. Ge, B. Jiang, Y. Jiang, J. Liu, T. Liu, C. Xue, Y. Ye and C. Zhang, An enhanced alternating direction method of multipliers-based interior point method for linear and conic optimization. INFORMS Journal on Computing, 37(2), pp.338-359 (2025).
[57] S. Jiang, B. Natura and O. Weinstein, A Faster Interior-Point Method for Sum-of-Squares Optimization. Algorithmica 85, 2843–2884 (2023). https://doi.org/10.1007/s00453-023-01112-4